Transient-Liquid-Phase bonding for Skutterudite-based thermoelectric modules

Christian Stiewe[1], Eckhard Müller[1,2]
[1] Institute of Materials Research, German Aerospace Center, 51170, Cologne, Germany
[2] Institute of Inorganic and Analytical Chemistry, Justus Liebig University Giessen, Heinrich-Buff-Ring 17, 35392, Giessen, Germany
Corresponding author: christian.stiewe@dlr.de
Keywords: thermoelectric; Skutterudite; module simulation; contact resistances
DOI: https://doi.org/10.1016/j.solidstatesciences.2023.107423

1. Abstract

Thermoelectric (TE) generators are an option for waste heat recovery in a large diversity of applications, such as automotive, aerospace or high temperature industrial processes with high energy throughput. Skutterudite materials are among the most interesting candidates for high efficiency modules in the high-temperature range up to 500 °C. However, Skutterudite-based TE modules still lack published results on reliable solutions for electrical and thermal contacts between the semiconducting TE pellets and metallic bridges and their stability under thermal treatment, leaving room for suggestions on durable joining and assembly technology.
In this article we will present contacting schemes for TE couples using different diffusion barriers and a transient liquid phase (TLP) joining process. The joints have been investigated concerning their microstructure, diffusion effects and electrical contact resistivities. $CrSi_2$ has shown suitable as anti-diffusion layer with good adhesion and electrical properties leading to contact resistivities as low as 5 $\mu\Omega\cdot cm^2$.

2. Introduction

Thermoelectric generators are used to convert flowing heat directly into electricity without moving parts or working fluids, thus providing a great potential in applications of waste heat recovery or energy harvesting [1, 2]. Waste heat in automotive and industrial processes is mostly provided at elevated temperatures beyond the limit of Bi_2Te_3-based modules of 250 °C. TE modules for the use in this high temperature range are scarcely commercially available, mainly because of the challenging task of establishing reliable contacts between the TE material and the metallic bridges. The requirements for these contacts are manifold, as they have to be mechanically stable under long-term and cycling thermal treatment, exhibit low thermal and electrical contact resistances and must not alter the TE materials´ properties.
Skutterudites are among the materials with highest conversion efficiency, given by the thermo-electric figure of merit ZT, in the relevant temperature range between 250 and 550 °C [3-6]. ZT a measure for a TE materials efficiency and is defined as $ZT=(S^2\sigma/\kappa)\cdot T$, with the Seebeck coefficient S, electrical conductivity σ, thermal conductivity κ and the absolute temperature T. Several setups for Skutterudite-based TE modules have been reported ([7]: power density up to 0.9 W/cm²; [8]: Eta 7.27%; [9]: Eta 8%; [10]: up to 2.1 W/cm²; [11]: Eta 9.15%) with achieved conversion efficiencies of up to 8% and 9.15% at a temperature gradient of 550 K and 600 K, respectively. For the module setup metal electrodes were sintered to the TE material before contacting to the metal bridges and serve as diffusion barriers.
The conventional TE device manufacturing uses brazing to join the functionalized single legs to the metallic bridges, which is limited by the thermal stability up the braze´s re-melting point and possible extensive growth of reaction layers at the interfaces. Designing a suitable metallization and bonding technique for the Skutterudite family of compounds is particularly difficult with the complex reactivity of their individual components, since antimony (Sb) can react with most of the transition metals to form brittle antimonide intermetallic compounds (IMCs). The transient liquid phase (TLP) bonding (also known as solid liquid interface diffusion SLID) allows to overcome the issue of producing a joint without affecting the Skutterudite integrity as a consequence of high process

temperatures [12, 13]. The basics of the TLP process is described by MacDonald et.al. [14] and well known for different metal combinations, such like Ag-In, Au-In, Cu-In [15] or Cu-Sn and Ni-Sn [16]. Placha et.al. report on the contacting of p-type Skutterudite materials using an Al-Ni-based TLP bonding process with electroless Ni-plating and introducing a 17 µm thick Al foil [17]. Contacts with high shear strengths of 4.5-5.1 MPa and contact resistivities in the range of 28-48 $\mu\Omega\cdot cm^2$ were obtained.
In this study focusses on functionalized TE single legs and couples that were set up using a Co-Sn-based TLP bonding technique in combination with diffusion barrier coatings on p- and n-type Skutterudite pellets. The diffusion reaction-controlled process leads to the formation of IMCs, CoSn and $CoSn_2$, with theoretical melting points above the joining and addressed application temperature. Metals like Mo, W and Cr are interesting candidates for diffusion barriers, but are not suitable for application with Skutterudite materials due to their hardness in combination with a mismatch in the coefficient of thermal expansion (CTE, see Table 1) leadings to cracks and delamination. Metal silicides, as used as diffusion barriers in semiconductor processing [18], present an interesting alternative and are known as coatings for various applications, like in case of $MoSi_2$ [19] or $FeSi_2$ [20] as oxidation protection for Mg_2Si. Three metal silicides with attractive properties like high melting point, low electrical resistance and high-temperature chemical stability have been tested in this study: $MoSi_2$ [21], $TiSi_2$ [22] and $CrSi_2$ [23]. These compounds have been applied as diffusion barriers on Skutterudite legs by magnetron sputtering.
A large mismatch in the CTE should generally be avoided for reduced thermo-mechanical stress inside such contacts. In case of brittle materials of the contacted partners this requirement is more severe than for ductile materials. Skutterudites and most silicides are known to be brittle, hence matching CTEs determined the choice of materials here. The CTE of the Cu/Sn/Co system as joining partner depends strongly on the actual composition, for the Cu-Sn system ranging between $16.5\cdot10^{-6}$ and $22\cdot10^{-6}$ K^{-1} with reduced values by the addition of Co. While a Co addition typically also changes the hardness of a composition, it can be expected that the Cu/Sn/Co phases in the contacts will remain more ductile than brittle, leading to a broader range of reasonable CTEs.
Microstructures and electrical resistivities of the contacts have been investigated.

Table 1: CTE of different materials taken from a: [24] (values depend on composition); b: [25]; c: [26]; d: [27]

	n-Skd[a]	p-Skd[a]	W[b]	Mo[b]	Ti[b]	Cr[b]	$MoSi_2$[c]	$TiSi_2$[d]	$CrSi_2$[d]
CTE [$10^{-6}K^{-1}$]	~9.5	~11.5	4.5	5.4	8.6	5.9	8.1	9.6	10.5

3. Materials and Methods

The Skutterudite materials under investigation have been either prepared by gas atomization using a Hermiga 75 Mini by Phoenix Scientific Instruments, Great Britain, in the nominal composition $In_{0.25}Co_4Sb_{12}$ (n-type) and $Ce_{0.4}Nd_{0.4}Fe_{3.7}Ni_{0.3}Sb_{12}$ (p-type) or received from Treibacher Industry AG, Austria, as $CoSb_3$-based (n-type) and $(Fe,Co)Sb_3$-based (p-type) materials. The powder fabrication by gas atomization allows for the production of up to 3 kg of material per batch under an Ar atmosphere. The resulting powders have mostly spherical particles with sizes around 10 µm. While the as-atomized powders do hardly consist of the Skutterudite phase, this desired phase is almost completely formed during the hot-pressing step, because of the micro-scaled phase distribution. The details of the powder fabrication by gas atomization can be found elsewhere [28]. Powders were compacted in a graphite pressing die with a diameter of 50 mm using a current-assisted hot press (Dr. Fritsch DSP 510A) at 655 °C under 60 MPa in vacuum. The discs were grinded and cut into bars for TE characterization and legs for contacting tests and module setup using a wafer saw DAD321 by Disco, Japan.
The temperature-dependent thermal conductivity is calculated from the thermal diffusivity measured with a Netzsch LFA 427, Archimedes' density, and specific heat calculated for the materials´ composition following Dulong-Petit´s law. The temperature-dependent electrical

conductivity σ and Seebeck coefficient *S* were measured simultaneously using a custom-built measurement device [29]. S and σ are recorded during subsequent heating and cooling phases of the measurement cycle to obtain information on the functional material stability. Measurement errors are assumed to be 8%, 5%, and 5% for κ, *S*, and σ, respectively. The repeatability of the Seebeck coefficient measurement is better than 5% allowing for the identification of smaller differences between samples; the 5% error mainly accounts for accuracy, meaning an absolute uncertainty of the measured values due to systematic errors [30]. These values sum up to an accuracy of the calculated figure of merit of approx. 20%.
Metal layers on Cu bridges and on the TE legs have been established by galvanic coating or physical vapor deposition using an AXPLORER 4375 S3E1 by AxynTeC Dünnschichttechnik GmbH, equipped with three DC magnetron sputtering sources and an electron beam evaporation system. Various targets have been used for the different coatings, such as Co, Ti, Sn, $MoSi_2$, $TiSi_2$ and $CrSi_2$ (all Evochem Advanced Materials GmbH). Sn as a component for the TLP bonding has been introduced as a foil (Goodfellow, Cambridge, UK, 99.9% purity), by galvanic or by PVD coating. Microstructural investigations have been done using a Zeiss Ultra 55 SEM in combination with an Oxford EDX detector. The quality of the contacts was estimated by the voltage profiles across the joints and the preservation of the Seebeck coefficient of the TE material using a Potential & Seebeck Scanning Microprobe (PSM) [31].

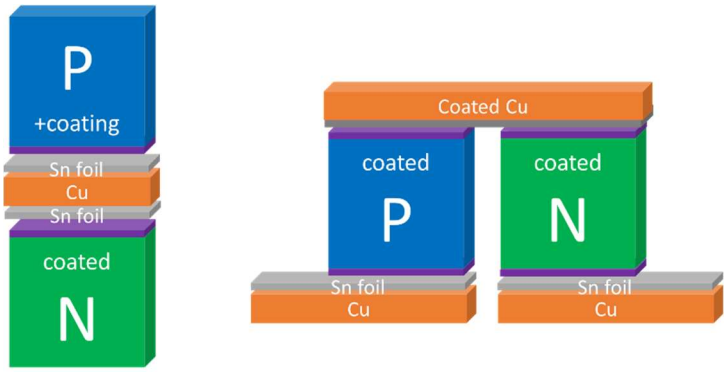

Figure 1: Sketches of the tested joining setups as piles (left) and unicouples (right) of functionalized TE legs to Cu bridges

TE piles and unicouples have been prepared by joining of functionalized TE legs to Cu (see Figure 1) under controlled conditions like temperature, axial load and atmosphere using an in-house-built induction furnace.

4. Results and Discussion

TE material
The Seebeck coefficient, the thermal and electrical conductivity for the material synthesized at DLR and provided by TIAG have measured in the range between 25 and 500 °C. These data are used as input for the 1D and 3D simulation of unicouples set up using these materials. The The figure of merit was calculated as well and is presented in Figure 2. Higher ZT values for both n- and p-type material is obtained for the TIAG material, which is promising for higher module efficiencies. Micrographs of the hot-pressed materials revealed a smaller residual porosity for the TIAG material, especially for the n-type samples. For these reasons the contacting experiments have mainly been performed using the TIAG material.

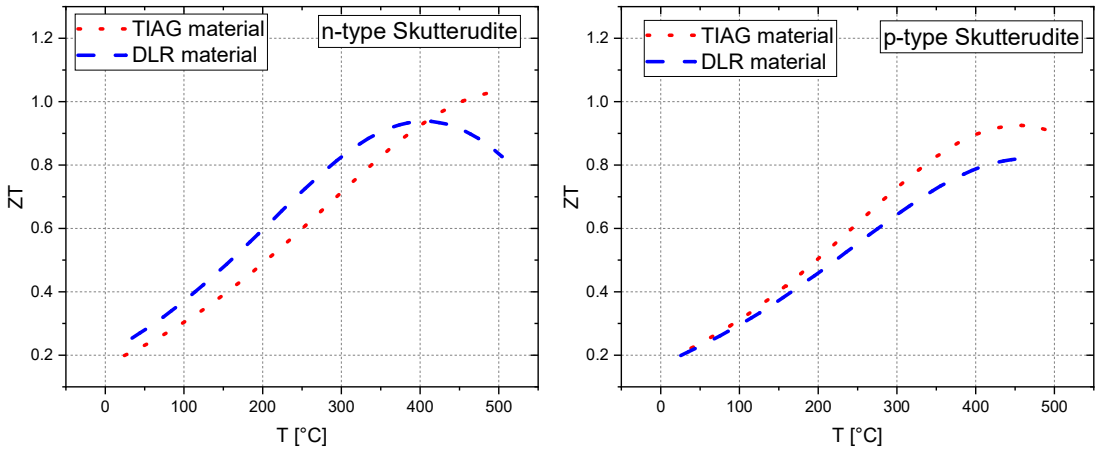

Figure 2: ZT values calculated from measured TE properties of TIAG material compacted at DLR and material synthesized at DLR.

Diffusion barriers

In a first joining test no diffusion barrier was used, but a Co layer of 0.25 µm thickness was sputtered directly on the contact surface of the Skutterudite legs. For the contact to 0.15 mm thick Cu electrodes a Sn foil with a thickness of 12.5 µm was used. The setup was heat treated for 30 min at 550 °C under 0.3 bar of Ar and an axial pressure of 4 MPa.

Figure 3 shows SEM micrographs after the contacting test. A significant diffusion of Cu into the Skutterudite can be seen, which is slightly more pronounced in the p-type compared to the n-type material (190 µm compared to 160 µm). Additionally, cracks in both TE legs can be observed perpendicular to the contacting surface, probably as a result of a CTE mismatch between TE material and IMC.

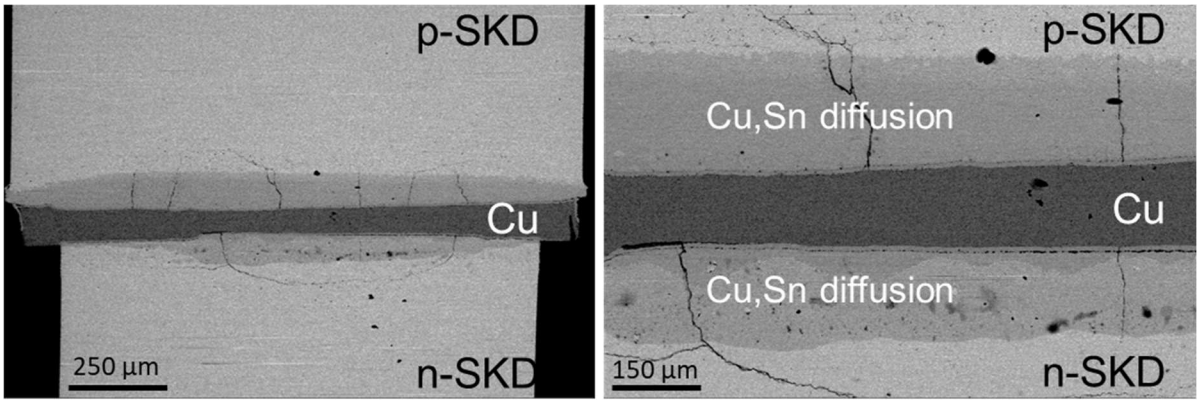

Figure 3: SEM micrographs of p- and n-type Skutterudite legs without diffusion barrier after contacting to Cu.

These results show the necessity for a diffusion barrier to protect the TE material from the diffusion of Cu and Sn. Metal silicides are known for their use as protection layer against oxidation, e.g. on Mg_2Si materials. Their high electrical conductivity in combination with CTE values close to those of Skutterudites make some metal silicides interesting candidates as diffusion barriers.

Therefore $MoSi_2$, $TiSi_2$ and $CrSi_2$ layers with initial thickness of 1.5 µm have been applied by PVD to the contacting surface of the Skutterudite legs before subsequent coating with Co and Sn. Figure 4 shows the microstructure of the contacting areas after joining to Cu. Gap-free contacts could be established and the reaction zone of Sn, Co and Cu is clearly visible. In the higher magnification cracks in the $MoSi_2$ layer become visible that are filled with a mixture of Cu, Sn and Sb. Obviously the $MoSi_2$ layer broke during heating, because of its lower CTE, so the gaps could fill with (Cu,Sn) and react with the Sb of the Skutterudite. A Cu-rich phase is clearly visible between the $MoSi_2$ and Skutterudite, proofing that $MoSi_2$ failed as diffusion barrier in this process.

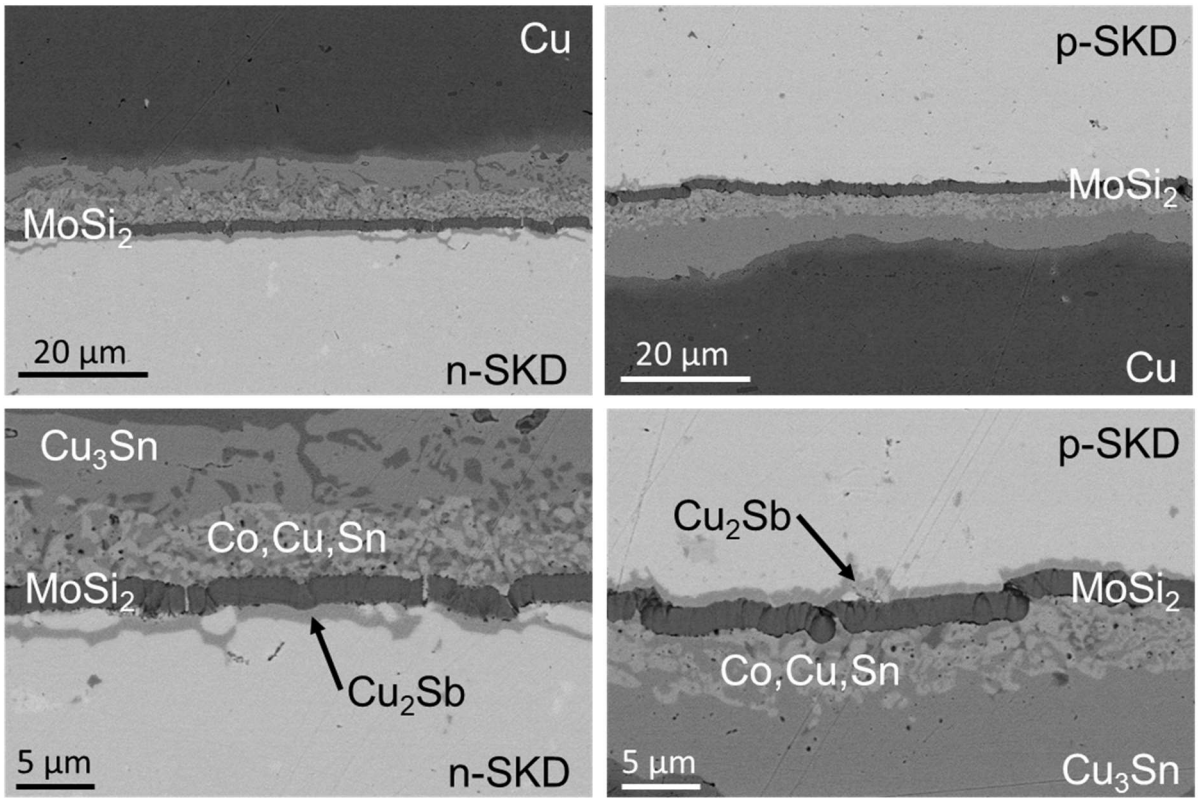

Figure 4: SEM micrographs of a Skutterudite-Cu-pile using $MoSi_2$ as diffusion barrier after contacting at different magnifications (left: n-type; right: p-type)

The results of the microstructure investigation on the joint Skutterudites using $TiSi_2$ as diffusion barrier can be seen in Figure 5. Again gap-free contacts could be achieved and no obvious cracks were found in the $TiSi_2$ layer. Still a significant Cu diffusion into the Skutterudite could be observed in extended zones compared to the $MoSi_2$ joints leading to the formation of Cu_2Sb. This diffusion is significantly stronger in the n-type compared to the p-type material. The EDX analysis in different locations of the $TiSi_2$ layer varying high contents of Cu inside this layer as well as a partly of $TiSi_2$ into TiSi. Such a transition is not to expect at temperatures around 550 °C, since both TiSi and $TiSi_2$ are high temperature phases with decomposition temperatures at 1480 °C and 1330 °C, respectively. A more detailed investigation of the $TiSi_2$ coating on the TE material before contacting shows a seemingly homogeneous phase on the µm scale, but the EDX analysis suggests a composition of Ti:Si = 2:3. Since the Ti-Si phase diagram does not show an according phase it must be assumed that the expected $TiSi_2$ coating is a mixture of TiSi and $TiSi_2$ phases on a sub-µm scale that encounters some grain growth during heat treatment for the joining test. The presence of grain boundaries than allows for the diffusion of Cu, Sn and Sb as detected in micrographs.

Tests with $CrSi_2$ coatings directly on the Skutterudite legs showed very poor adhesion after the heat treatment for contacting. The Cu contact were mechanically more fragile with the n-type material compared to the p-type. SEM micrographs of the broken contacts showed a separation mainly between the TE material and the $CrSi_2$ layer, making the introduction of an adhesion promoter necessary. Ti and Co layers, respectively, have been introduced by magnetron sputtering on the Skutterudite legs prior to the $CrSi_2$ coating. These samples showed fairly mechanically stable contacts after joining to Cu. For Ti as adhesion promoter the microstructure investigations revealed a strong Cu diffusion into the TE material with the formation of Cu_2Sb and was not pursuit further.

Ti as adhesion promoter possibly failed because of a formation of TiSi and $TiSi_2$, both having lower formation enthalpies (-72.6 and -57.0 kJ/mol, respectively, [32]) compared to $CrSi_2$ (-25.8 kJ/mol). Such a partly transition of $CrSi_2$ into CrSi could cause diffusion along the grain boundaries similar to the observation with $TiSi_2$ as diffusion barrier. Another possible explanation might be a diffusion of Ti

through the $CrSi_2$ layer and a reaction with Cu and Sn, because CuSnTi exhibits an eutectic melting point at slightly below 550 °C [33].

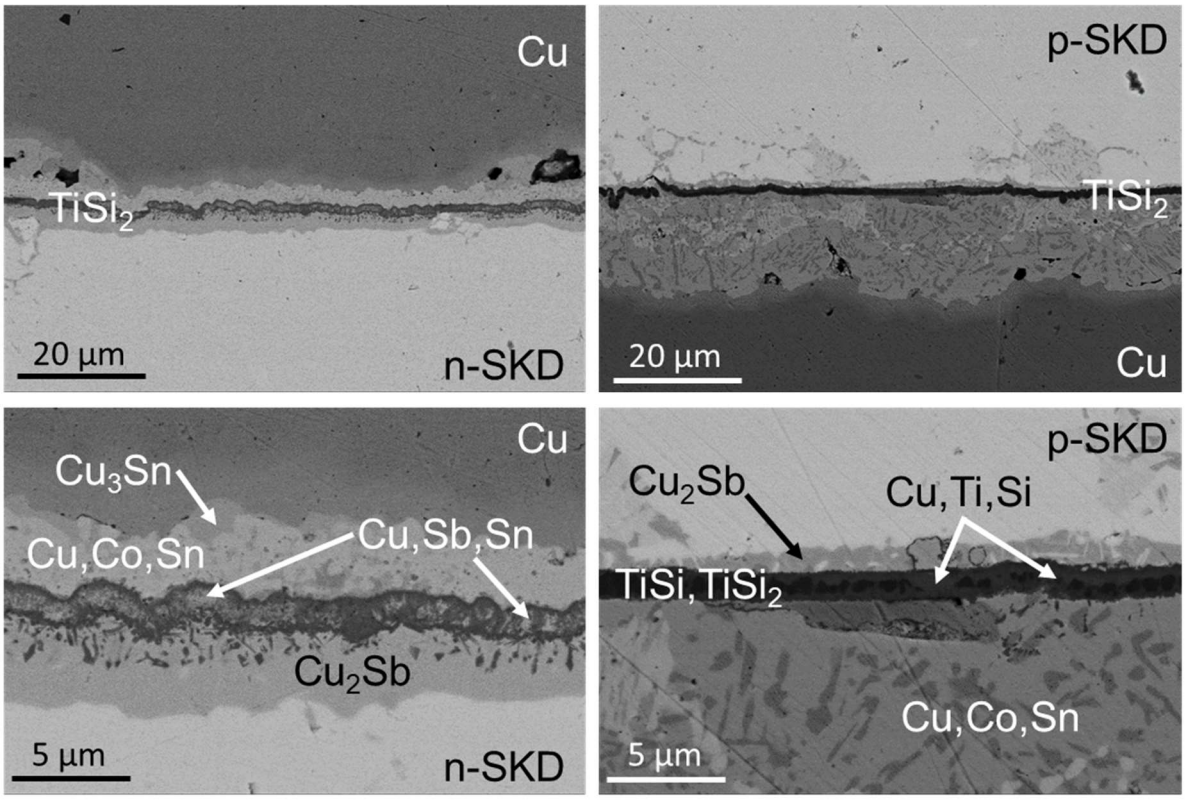

Figure 5: SEM micrographs of a Skutterudite-Cu-pile using $TiSi_2$ as diffusion barrier after contacting at different magnifications (left: n-type; right: p-type)

The microstructure and line scans obtained after contacting of the TE samples using Co as adhesion promoter are presented in Figure 6. Magnetron sputtering of Co allows for only very low deposition rates, because of the magnetic properties of Co. Hence, to achieve Co layers of 1.5 µm electron beam evaporation has been used, leading the deposition of porous Co layers on both sides of the $CrSi_2$ diffusion barriers. The reaction zones between Cu, Co and Sn can be seen on the TLP side and a reaction between the Co of the adhesion promoter layer and the n- and p-type Skutterudite, respectively, forming a CoSb phase in the first and a $(Co,Fe)Sb_2$ phase in the latter case. These findings present the state after the heat treatment of 30 min at 550 °C. It can be assumed that the reaction between the Co layers an Sn/Cu on one side and p-type or n-type Skutterudite on the other will slowly progress in long-term annealing at application temperature, until the Co layers are completely consumed. This will lead to an increased thickness of the CoSb- and $CoSb_2$-phases, reducing the TE effective length of the Skutterudite legs. To overcome negative effects on module performance, the Co layer as adhesion promoter should be of reduced thickness.
No Cu is detected in the TE material as well as no Sb in the Cu contact, proving the functionality of the $CrSi_2$ layer as diffusion barrier. The peaks of unreacted Co are visible on both sides of the $CrSi_2$ layer. The formation enthalpies of Co-Si phases with -49.3 kJ/mol for CoSi and -34.3 kJ/mol for $CoSi_2$ [34] are lower compared to $CrSi_2$. The recorded line scans do not provide clear evidence, nevertheless the formation of thin Co-Si pahse can be assumed between the Co and the $CrSi_2$ layer, leading to an improved adhesion compare to $CrSi_2$ coated directly on Skutterudite.

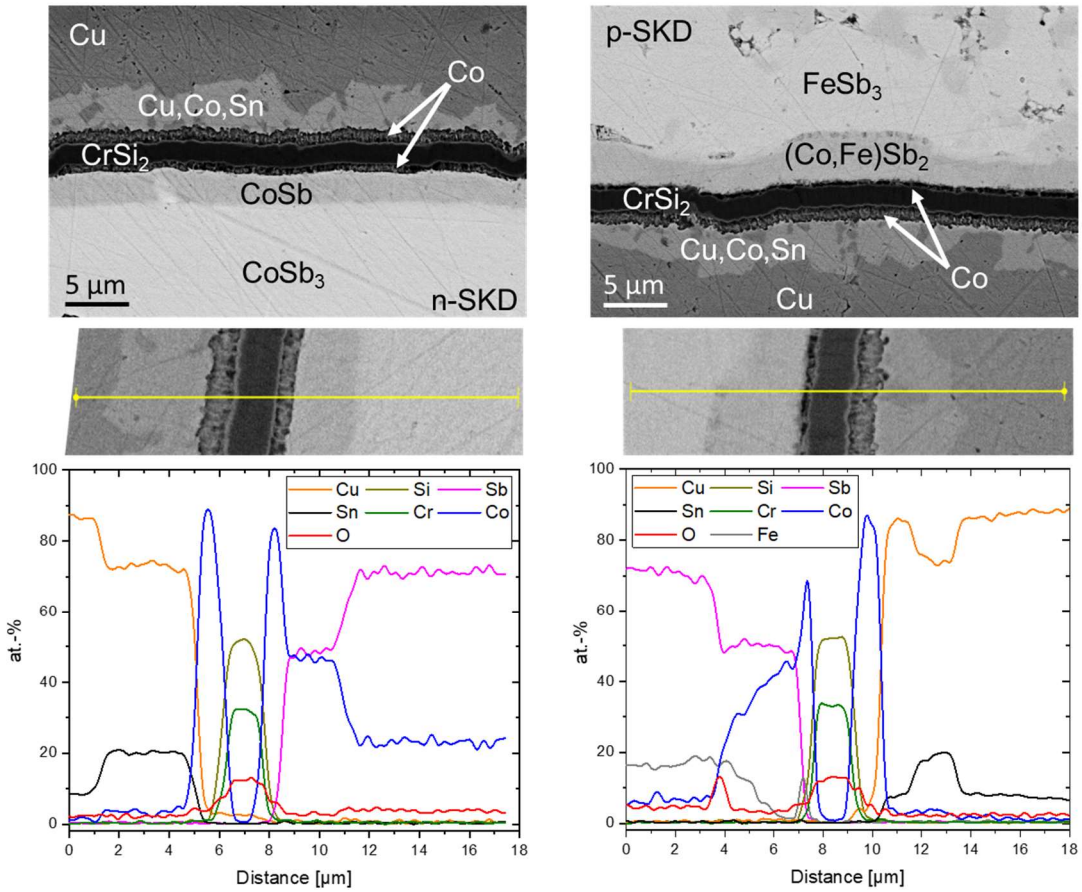

Figure 6: SEM micrographs and EDX line scans of a Skutterudite-Cu-pile using $CrSi_2$ as diffusion barrier and Co as adhesion promoter after contacting at different magnifications (left: n-type; right: p-type)

TE couples

In a step towards module fabrication single TE legs have been contacted on one side by the established TLP technique, serving as hot side, and by simple Sn soldering on the other, the cold side. These samples have been investigated for their electrical contact resistances at room temperature by a Potential Seebeck Microprobe (PSM). The scanning step for the contact resistivity measurement can be varied in a broad range with a minimum scan length of 1 µm as given by the LINOS linear stages. For the presented results a scanning step of 50 µm was used as a compromise between spatial resolution and measurement duration (approx. 10 sec per combined measurement of electrical and thermal voltages). 5 lines have been scanned over the width of the leg and averaged. Figure 7 shows line scans for the Seebeck coefficient and the electrical potential for the contacted n- and p-type samples, respectively. The plateaus in the electrical potential represent the high electrical conductivity of the Cu electrodes. The difference in the electrical potential ΔU_{Pot} at the hot and cold side contacts is used to calculate the specific contact resistances ρ_C. No significant step in the $U_{Pot}(x)$ profile can be identified and the calculated values for ρ_C remained below 5 $\mu\Omega\cdot cm^2$ for all line scans over the width of the contacts.

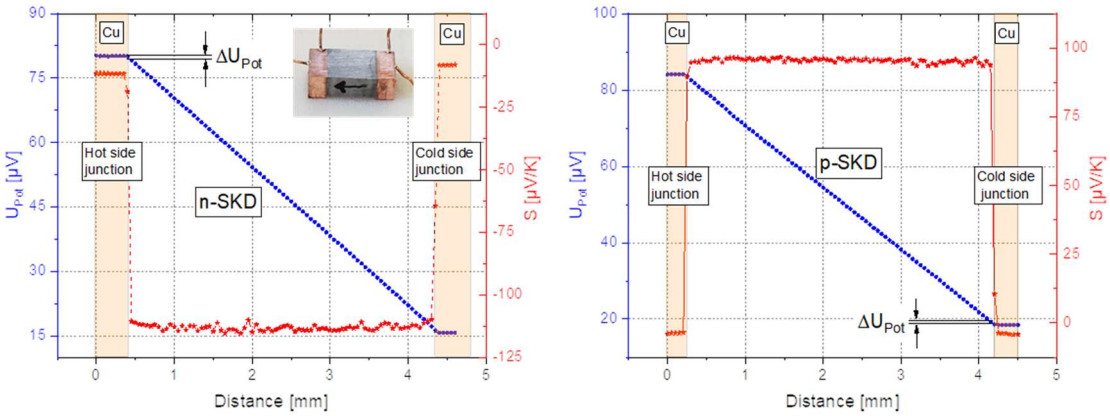

Figure 7: Line scans of the Seebeck coefficient (red) and electrical potential (blue) for Cu contacted n-type (left) and p-type (right) Skutterudite single legs; inset: picture of a contacted single leg

5. Conclusion

Co-Sn based transient liquid phase bonding was investigated as contacting technique for joints between p- and n-type Skutterudite legs and Cu bridges. The metallization was mainly established by DC magnetron sputtering. The necessity of a diffusion barrier was shown to suppress the diffusion of Cu and Sb into the Skutterudite and the bridges. $MoSi_2$, $TiSi_2$ and $CrSi_2$ were tested as possible candidates for diffusion barriers. After heat treatment for the joining process the $MoSi_2$ layer showed cracks leading to diffusion of Cu and Sn, while the $TiSi_2$ layer transformed into a mixture of TiSi and $TiSi_2$ phases and findings of Cu and Sn inside the Ti silicide layer as well as in the Skutterudite, presumably because of diffusion along grain boundaries of the Ti silicide phases.
$CrSi_2$ showed very poor adhesion to the Skutterudites leading to delamination and separation of the Cu electrodes from the TE legs. The introduction of Ti or Co was tested as adhesion promoters between Skutterudite and $CrSi_2$. Ti showed a strong reaction with $CrSi_2$ with the formation of Ti silicides and causing the failure of $CrSi_2$ as diffusion barrier. A reaction of Co to Co-Si phases could not be observed possibly because of the layer thickness and a limited spatial resolution of the EDX system. The formation of Co-Si is very likely from the view of formation enthalpies and would explain the significantly improved adhesion of the $CrSi_2$ layer. No Cu and/or Sn diffusion was observed for this contacting scheme.
Measurements of the electrical contact resistivities on contacted single legs showed no significant voltage drops at the contacts resulting in very low ρ_c values below 5 $\mu\Omega/cm^2$. First tests of the durability of the joints have been done up to 100 h in a constant temperature gradient of 500 °C on the hot side and 50 °C on the cold side without significant change in the measured total electrical resistance. Detailed tests for long-term thermal stability are necessary and ongoing.

6. Acknowledgements

The authors would like to thank Dipl.-Ing. P. Blaschkewitz for TE characterization of materials and modules.

7. Literature

1. *Thermoelectrics Handbook: Macro to Nano* 1ed, ed. D.M. Rowe. 2005, Boca Raton: CRC Press, Taylor & Francis. 1008.

2. Champier, D., *Thermoelectric generators: A review of applications.* Energy Conversion and Management, 2017. **140**: p. 167-181.
3. Rull-Bravo, M., et al., *Skutterudites as thermoelectric materials: revisited.* RSC Advances, 2015. **5**(52): p. 41653-41667.
4. Sales, B.C., *Filled Skutterudites*, in *Handbook on the Physics and Chemistry of Rare Earths*, J.C.G.B. K.A. Gschneidner and V.K. Pecharsky, Editors. 2003, Elsevier: online. p. 1-34.
5. Biswas, K., et al., *High-performance bulk thermoelectrics with all-scale hierarchical architectures.* Nature, 2012. **489**: p. 414-418.
6. Rogl, G. and P. Rogl, *Skutterudites, a most promising group of thermoelectric materials.* Current Opinion in Green and Sustainable Chemistry, 2017. **4**(Supplement C): p. 50-57.
7. Prado-Gonjal, J., et al., *Skutterudite Thermoelectric Modules with High Volume-Power-Density: Scalability and Reproducibility.* ACS Applied Energy Materials, 2018. **1**(11): p. 6609-6618.
8. Li, W., et al., *High-Efficiency Skutterudite Modules at a Low Temperature Gradient.* energies, 2019. **12**(22): p. 4292.
9. Guo, J.Q., et al., *Development of Skutterudite Thermoelectric Materials and Modules.* Journal of Electronic Materials, 2012. **41**(6): p. 1036-1042.
10. Park, S.H., et al., *High-Power-Density Skutterudite-Based Thermoelectric Modules with Ultralow Contact Resistivity Using Fe–Ni Metallization Layers.* ACS Applied Energy Materials, 2018. **1**(4): p. 1603-1611.
11. Nie, G., et al., *High performance thermoelectric module through isotype bulk heterojunction engineering of skutterudite materials.* Nano Energy, 2019. **66**: p. 104193.
12. Cook, G.O. and C.D. Sorensen, *Overview of transient liquid phase and partial transient liquid phase bonding.* Journal of Materials Science, 2011. **46**(16): p. 5305-5323.
13. Jung, D.H., et al., *A Review on Recent Advances in Transient Liquid Phase (TLP) Bonding for Thermoelectric Power Module.* REVIEWS ON ADVANCED MATERIALS SCIENCE, 2018. **53**(2): p. 147-160.
14. W D MacDonald, a. and T.W. Eagar, *Transient Liquid Phase Bonding.* 1992. **22**(1): p. 23-46.
15. Bernstein, L., *Semiconductor Joining by the Solid-Liquid-Interdiffusion (SLID) Process.* Journal of The Electrochemical Society, 1966. **113**(12): p. 1282.
16. Chu, K., Y. Sohn, and C. Moon, *A comparative study of Cu/Sn/Cu and Ni/Sn/Ni solder joints for low temperature stable transient liquid phase bonding.* Scripta Materialia, 2015. **109**: p. 113-117.
17. Placha, K., et al., *Solid-Liquid Interdiffusion (SLID) Bonding of p-Type Skutterudite Thermoelectric Material Using Al-Ni Interlayers.* Materials (Basel, Switzerland), 2018. **11**(12): p. 2483.
18. Ohring, M., *Chapter 11 - Interdiffusion, Reactions, and Transformations in Thin Films*, in *Materials Science of Thin Films (Second Edition)*, M. Ohring, Editor. 2002, Academic Press: San Diego. p. 641-710.
19. Battiston, S., et al., *Multilayered thin films for oxidation protection of Mg2Si thermoelectric material at middle–high temperatures.* Thin Solid Films, 2012. **526**: p. 150-154.
20. Tani, J.-i., M. Takahashi, and H. Kido, *Fabrication of oxidation-resistant β-FeSi2 film on Mg2Si by RF magnetron-sputtering deposition.* Journal of Alloys and Compounds, 2009. **488**(1): p. 346-349.
21. Yamada, T. and H. Yamane, *Crystal structure and thermoelectric properties of β-MoSi2.* Intermetallics, 2011. **19**(7): p. 908-912.
22. Hilleringmann, U., M. Schönhoff, and F. Assion. *Titanium disilicide as hot side metallization layer for thermoelectric generators*. in *2013 Africon*. 2013.
23. Dasgupta, T., et al., *Structural, thermal, and electrical properties of CrSi2.* 2008. **103**(11): p. 113516.
24. Rogl, G., et al., *Thermal expansion of skutterudites.* Journal of Applied Physics, 2010. **107**: p. 043507-043507.

25. ToolBox, E. *Thermal Expansion of Metals*. 2005; Available from: https://www.engineeringtoolbox.com/thermal-expansion-metals-d_859.html.
26. Fu, Q.-G., et al., *B2O3 modified SiC–MoSi2 oxidation resistant coating for carbon/carbon composites by a two-step pack cementation.* Corrosion Science, 2009. **51**(10): p. 2450-2454.
27. Raj, S.V., *Comparison of the Thermal Expansion Behavior of Several Intermetallic Silicide Alloys Between 293 and 1523 K.* Journal of Materials Engineering and Performance, 2015. **24**(3): p. 1199-1205.
28. Stiewe, C., et al., *Upscaled Synthesis of n- and p-type Thermoelectric Skutterudite single legs by Gas Atomization and Current-assisted Sintering.* Physica Status Solidi A: Applications and Materials Science, 2018.
29. de Boor, J., et al., *High-Temperature Measurement of Seebeck Coefficient and Electrical Conductivity.* Journal of Electronic Materials, 2013. **42**(7): p. 1711-1718.
30. de Boor, J. and E. Muller, *Data analysis for Seebeck coefficient measurements.* Review of Scientific Instruments, 2013. **84**(6): p. 065102.
31. Ziolkowski, P., et al., *Potential & Seebeck Microprobe – Imaging of electrical and thermoelectric material properties on the microscale*, in *DPG Frühjahrstagung*. 2009: Dresden.
32. Meschel, S. and O. Kleppa, *Thermochemistry of Alloys of Transition Metals and Lanthanoid Metals with Some IIIB and IVB Elements in the Periodic Table.* Journal of Alloys and Compounds - J ALLOYS COMPOUNDS, 2001. **321**: p. 183-200.
33. Zhou, G.-j., Y. Zhou, and Y. Luo, *Phase equilibria of the Cu-Sn-Ti ternary system at 823K.* 2017. **7**(2): p. 025118.
34. Vantomme, A., et al., *Concentration-controlled phase selection of silicide formation during reactive deposition.* Applied Physics Letters, 1999. **74**: p. 3137-3139.